FOUNDATIONS ADVANCES

ISSN 2053-2733

Icosahedral symmetry breaking: C_{60} to C_{84}, C_{108} and to related nanotubes

Mark Bodner,[a] Emmanuel Bourret,[b] Jiri Patera[a,b] and Marzena Szajewska[a,b,c]*

[a]MIND Research Institute, 111 Academy Drive, Irvine, California 92617, USA, [b]Centre de Recherches Mathématiques, Université de Montréal, C. P. 6128, Centre-ville, Montréal, H3C 3J7, Québec, Canada, and [c]Institute of Mathematics, University of Bialystok, 1M Ciolkowskiego, PL-15-245, Bialystok, Poland. *Correspondence e-mail: m.szajewska@math.uwb.edu.pl

Received 11 November 2014
Accepted 24 February 2015

Edited by W. F. Kuhs, Georg-August University Göttingen, Germany

Keywords: finite Coxeter group; symmetry breaking; fullerenes; nanotubes.

This paper completes the series of three independent articles [Bodner *et al.* (2013). *Acta Cryst.* A**69**, 583–591, (2014), *PLOS ONE*, 10.1371/journal.pone.0084079] describing the breaking of icosahedral symmetry to subgroups generated by reflections in three-dimensional Euclidean space $\mathbb{R}^3$ as a mechanism of generating higher fullerenes from C_{60}. The icosahedral symmetry of C_{60} can be seen as the junction of 17 orbits of a symmetric subgroup of order 4 of the icosahedral group of order 120. This subgroup is noted by $A_1 \times A_1$, because it is isomorphic to the Weyl group of the semi-simple Lie algebra $A_1 \times A_1$. Thirteen of the $A_1 \times A_1$ orbits are rectangles and four are line segments. The orbits form a stack of parallel layers centered on the axis of C_{60} passing through the centers of two opposite edges between two hexagons on the surface of C_{60}. These two edges are the only two line segment layers to appear on the surface shell. Among the 24 convex polytopes with shell formed by hexagons and 12 pentagons, having 84 vertices [Fowler & Manolopoulos (1992). *Nature (London)*, **355**, 428–430; Fowler & Manolopoulos (2007). *An Atlas of Fullerenes*. Dover Publications Inc.; Zhang *et al.* (1993). *J. Chem. Phys.* **98**, 3095–3102], there are only two that can be identified with breaking of the H_3 symmetry to $A_1 \times A_1$. The remaining ones are just convex shells formed by regular hexagons and 12 pentagons without the involvement of the icosahedral symmetry.

1. Introduction

In this paper, icosahedral symmetry and its implementation in the case of the fullerene C_{60} (see Fig. 1) is only briefly described, as its detailed exposition was presented in the two previous articles of the series (Bodner *et al.*, 2013, 2014) together with all notations.

The icosahedral group, denoted here by H_3, is of order 120. It is generated by three reflections, r_1, r_2, r_3, in the real Euclidean space $\mathbb{R}^3$. The simple roots α_1, α_2 and α_3 of H_3 are the normal vectors to the three reflection mirrors that meet at the origin and that define the icosahedral symmetry. They form the α-basis of the Euclidean space $\mathbb{R}^3$. A concise way to provide relative angles and a conventional choice of the lengths of the normals (Champagne *et al.*, 1995) is to define the matrix C of their scalar products $\langle \alpha_j, \alpha_k \rangle$. In the case of H_3, one has

$$C(H_3) = (\langle \alpha_j, \alpha_k \rangle) = \begin{pmatrix} 2 & -1 & 0 \\ -1 & 2 & -\tau \\ 0 & -\tau & 2 \end{pmatrix}, \quad \tau = \tfrac{1}{2}(1 + 5^{1/2}).$$

The ω-basis, reciprocal to α, is defined by

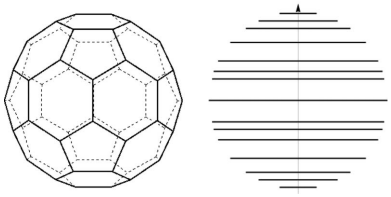

$$\langle \alpha_j, \omega_k \rangle = \delta_{jk}, \quad j,k = 1,2,3. \tag{1}$$

Specifically we get the relations between the basis vectors,

$$\begin{aligned}
\alpha_1 &= 2\omega_1 - \omega_2 & \omega_1 &= (1+\tfrac{1}{2}\tau)\alpha_1 + (1+\tau)\alpha_2 + (\tfrac{1}{2}+\tau)\alpha_3 \\
\alpha_2 &= -\omega_1 + 2\omega_2 - \tau\omega_3 & \omega_2 &= (1+\tau)\alpha_1 + (2+2\tau)\alpha_2 + (1+2\tau)\alpha_3 \\
\alpha_3 &= -\tau\omega_2 + 2\omega_3 & \omega_3 &= (\tfrac{1}{2}+\tau)\alpha_1 + (1+2\tau)\alpha_2 + (\tfrac{3}{2}+\tfrac{3}{2}\tau)\alpha_3.
\end{aligned} \tag{2}$$

In this paper, in addition to the α- and ω-bases, it is convenient to use the mixed basis $\{\omega_1, \alpha_2, \omega_3\}$ because, according to equation (1), α_2 is orthogonal to the plane spanned by ω_1 and ω_3.

Suppose (a, b, c) is given relative to the basis $\{\omega_1, \omega_2, \omega_3\}$. In order to transform it to the basis $\{\omega_1, \alpha_2, \omega_3\}$, one proceeds as follows:

$$(a,b,c)\begin{pmatrix} 1 & 1+\tau & 0 \\ 0 & 2+2\tau & 0 \\ 0 & 1+2\tau & 1 \end{pmatrix} = (a, a+2b+c+(a+2b+2c)\tau, c). \tag{3}$$

Thus one gets the following specific transformations:

$$\begin{aligned}
&(1,1,0) \longrightarrow (1, 3+3\tau, 0), \\
&(0, -1-2\tau, 3\tau) \longrightarrow (0, -1-\tau, -3\tau), \ldots
\end{aligned}$$

The subgroup of interest to us here can be set up in H_3 in many equivalent ways. One of them is particularly transparent: two of the simple roots of H_3 that are orthogonal to each other can be adopted as the simple roots of $A_1 \times A_1$. Putting $\beta_1 = \alpha_1$ and $\beta_2 = \alpha_3$ we have

$$C(A_1 \times A_1) = (\langle \beta_p, \beta_q \rangle) = \begin{pmatrix} 2 & 0 \\ 0 & 2 \end{pmatrix}, \quad p,q = 1,2.$$

In the previous work we first considered the symmetry H_3 broken to the symmetry group H_2 that is generated by reflections r_2, r_3 (Bodner *et al.*, 2013), and second we considered the breaking of the H_3 symmetry to A_2, generated by the reflections r_1 and r_2 (Bodner *et al.*, 2014). In the present paper the unbroken symmetry group is generated by the reflections r_1 and r_3. It is the Weyl group of the semi-simple Lie group $SU(2) \times SU(2)$, or equivalently, of its semi-simple Lie algebra $A_1 \times A_1$. The order of the group is 4. Hence its orbits consist of four, two or one point(s). It is convenient to write the orbit points in the ω-basis reciprocal to the α-basis of simple roots.

Reduction of the points of any orbit of H_3, in particular the 60 points/vertices of the polytope C_{60}, is found as in Bodner *et al.* [2013, equation (11)]. In the list the vertices are given in the basis $\{\omega_1, \omega_2, \omega_3\}$. Only the dominant points that identify the orbits of the appropriate subgroup are pointed out.

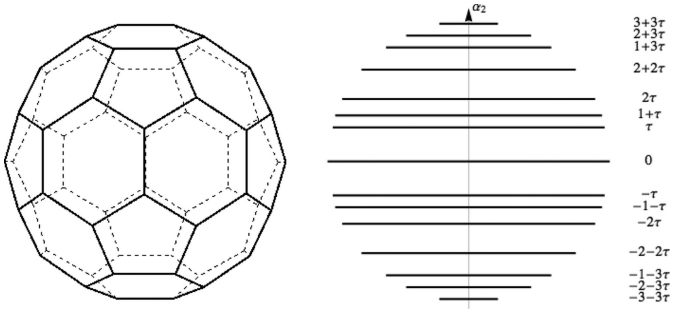

Figure 1
Two views of the polytope C_{60}. In one surface edges are shown. In the other only the orbits of $A_1 \times A_1$ are drawn as segments orthogonal to the axis of the polytope which is the simple root α_2. The last column of numbers contains coordinates of each $A_1 \times A_1$ orbit in the direction of α_2.

2. The $A_1 \times A_1$ orbits of vertices of C_{60}

There are two images of C_{60} in Fig. 1. The first one is done traditionally by showing the edges of the surface of the polytope and their intersections (vertices). The second image shows only the $A_1 \times A_1$ orbits. Since the polytope is oriented vertically along the α_2 axis, the $A_1 \times A_1$ orbits appear as segments, thus forming the 'stack of pancakes', with each $A_1 \times A_1$ orbit being just one 'pancake'.

The $A_1 \times A_1$-orbit structure of C_{60} becomes visible once the dominant points of each orbit are identified, which is simplified by working in the ω-basis of $\mathbb{R}^3$. Indeed, it suffices to find among the 60 vertices those that have non-negative first and third coordinates in the ω-basis, indicating a non-action of the reflections r_1 and r_3 on the corresponding vertex/point. Each $A_1 \times A_1$ orbit has precisely one dominant point; therefore it is specified by it.

The 60 vertices of C_{60} are given below in pairs that differ by an overall sign. If the sign of the first and third coordinate of a vertex coincide, one of the pair is a dominant point of an $A_1 \times A_1$ orbit. Boxes mark all such pairs in equation (4). If both the first and the third coordinates are positive, the orbit contains four points. If one of the coordinates is 0, the orbit is a segment with two vertices at its extremes. The following 60 vertices of C_{60} are written in the basis $\{\omega_1, \alpha_2, \omega_3\}$. The formula (3) applied to the 60 vertices in the ω-basis of Bodner *et al.* [2013, equation (11)] results in the following points in the basis $\{\omega_1, \alpha_2, \omega_3\}$:

$\boxed{\pm(1, 3+3\tau, 0)}$	$\boxed{\pm(2\tau, \tau, 2+\tau)}$	$\boxed{\pm(1+2\tau, 1+\tau, 2)}$
$\pm(-2-\tau, 2+2\tau, 1)$	$\pm(2+\tau, 2+2\tau, -1)$	$\boxed{\pm(-1, 3+3\tau, 0)}$
$\boxed{\pm(-1, 1+3\tau, -2\tau)}$	$\boxed{\pm(2+\tau, 2+2\tau, 1)}$	$\pm(1, 1+3\tau, -2\tau)$
$\pm(1+2\tau, 1+\tau, -2)$	$\boxed{\pm(2, 2+3\tau, \tau)}$	$\boxed{\pm(\tau, 2\tau, 1+2\tau)}$
$\boxed{\pm(-2\tau, \tau, -2-\tau)}$	$\pm(-1, 1+3\tau, 2\tau)$	$\pm(-2, 2+3\tau, \tau)$
$\boxed{\pm(1, 1+3\tau, 2\tau)}$	$\boxed{\pm(-2, 2+3\tau, -\tau)}$	$\boxed{\pm(-2-\tau, 2+2\tau, -1)}$
$\pm(\tau, 2\tau, -1-2\tau)$	$\pm(-2\tau, \tau, 2+\tau)$	$\boxed{\pm(3\tau, 0, 1)}$
$\boxed{\pm(0, \tau, 3\tau)}$	$\boxed{\pm(-\tau, 2\tau, -1-2\tau)}$	$\pm(-1-2\tau, 1+\tau, 2)$
$\pm(2\tau, \tau, -2-\tau)$	$\boxed{\pm(0, \tau, -3\tau)}$	$\boxed{\pm(-1-2\tau, 1+\tau, -2)}$
$\pm(-\tau, 2\tau, 1+2\tau)$	$\pm(3\tau, 0, -1)$	$\pm(2, 2+3\tau, -\tau)$

(4)

Thus there are 13 rectangular orbits,

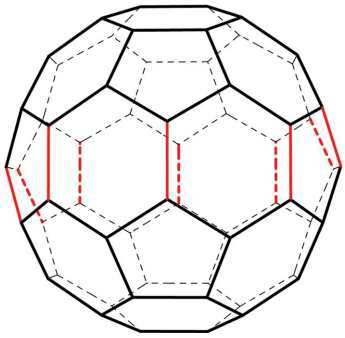

Figure 2
Coloured edges of C_{60} are to be removed before the insertion of additional spiral surface belts is undertaken. Removal of the edges also destroys four surface pentagons. They get replaced by four pentagons of the inserted spirals (Fig. 5).

$$\boxed{(2\tau,\tau,2+\tau)}\quad \boxed{(1+2\tau,1+\tau,2)}\quad \boxed{(1,-1-3\tau,2\tau)}$$
$$\boxed{(\tau,-2\tau,1+2\tau)}\quad \boxed{(2,2+3\tau,\tau)}\quad \boxed{(2\tau,-\tau,2+\tau)}$$
$$\boxed{(1+2\tau,-1-\tau,2)}\quad \boxed{(1,1+3\tau,2\tau)}\quad \boxed{(\tau,2\tau,1+2\tau)}$$
$$\boxed{(2,-2-3\tau,\tau)}\quad \boxed{(2+\tau,-2-2\tau,1)}\quad \boxed{(2+\tau,2+2\tau,1)}$$
$$\boxed{(3\tau,0,1)} \qquad (5)$$

and four orbits of two points,

$$\boxed{(1,3+3\tau,0)}\quad \boxed{(1,-3-3\tau,0)}\quad \boxed{(0,\tau,3\tau)}\quad \boxed{(0,-\tau,3\tau)} \qquad (6)$$

In order to find all the points of an $A_1 \times A_1$ orbit, it suffices to apply to the dominant points the transformation given in equation (5) and to the points given in equation (6) the reflections r_1 and r_3 in every way that yields a new point of the orbit.

The four orbits of two points.

$(1,1,0), r_1(1,1,0) = (-1,2,0)$
$(0,-1-2\tau,3\tau), r_3(0,-1-2\tau,3\tau) = (0,2+\tau,-3\tau)$
$(1,-2,0), r_1(1,-2,0) = (-1,-1,0)$
$(0,-2-\tau,3\tau), r_3(0,-2-\tau,3\tau) = (0,1+2\tau,-3\tau)$

Let us find the surface points of C_{60} with the direction of the axis of α_2 which is orthogonal to the plane spanned by ω_1 and ω_3. Clearly the points $(1,1,0)$ and $r_1(1,1,0) = (-1,2,0)$ are the end points of an edge on the top of C_{60} oriented as in Fig. 1. We have $\alpha_2 \sim (1,1,0) + (-1,2,0) = (0,3,0)$.

Let us view C_{60} as the stack of $A_1 \times A_1$ pancakes. For that we look at the vertices of C_{60} in the direction parallel to the plane spanned by ω_1 and ω_3. Then each $A_1 \times A_1$ orbit appears as a segment. If in addition no edges on the surface of C_{60} are shown, we have the 'pancake stack' of C_{60} that is oriented in the direction orthogonal to the plane of ω_1 and ω_3, or equivalently, to vector α_2 (see Fig. 1).

Both images of C_{60} in Fig. 1 display exact icosahedral symmetry, so that no symmetry breaking has occurred.

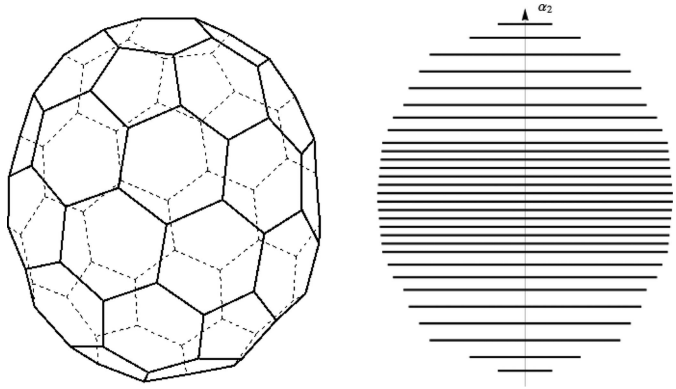

Figure 3
Pancake structure of C_{84}.

3. Symmetry breaking $C_{60} \rightarrow A_1 \times A_1$

In the previous two papers of this series, related cases were considered of breaking the icosahedral symmetry of $C_{60} \rightarrow H_2$ (Bodner *et al.*, 2013), and the symmetry breaking of C_{60} to A_2 (Bodner *et al.*, 2014). These cases can also be described as choosing a subgroup generated by selecting two of the three reflections r_1, r_2, r_3 generating H_3.

3.1. C_{84} from the $H_3 \rightarrow A_1 \times A_1$ symmetry breaking

The axis along which the symmetry breaking takes place in this paper is that of α_2. That is the reflections r_1 and r_3 remain as symmetry operations, while r_2 loses this role. The orbits of $A_1 \times A_1$ remain intact because they are in planes spanned by ω_1 and ω_3. In particular, the pancakes of Fig. 1 remain unchanged.

Symmetry breaking $C_{60} \longrightarrow A_1 \times A_1$ occurs in two steps:

(i) New orbits of $A_1 \times A_1$ are inserted into the C_{60} pancake stack.

(ii) Existing orbits of $A_1 \times A_1$ are displaced along the α_2 direction.

Both steps are subject to the additional constraint that the surface of the new polytope must be closed convex and formed by regular hexagons and 12 regular pentagons.

Both symmetry-breaking steps can be repeated any desired number of times.

Fig. 2 shows which edges of the polytope have to be removed before the insertion of new orbits is undertaken.

3.2. Inserted spirals

It remains to describe the orbits of $A_1 \times A_1$ that should be inserted into the stack of C_{60} in Fig. 1 so that it becomes the stack of C_{84} in Fig. 3.

This cannot be achieved here by insertion of one or several rings of hexagons into a surface of C_{60} as was the case (Bodner *et al.*, 2013, 2014). Here symmetry breaking is taking place through the insertion of one or several spiral loops of hexagons. Since a spiral can be left- or right-hand oriented in $\mathbb{R}^3$, there are two versions for each new polytope. In Fig. 4 both versions of C_{84} are shown.

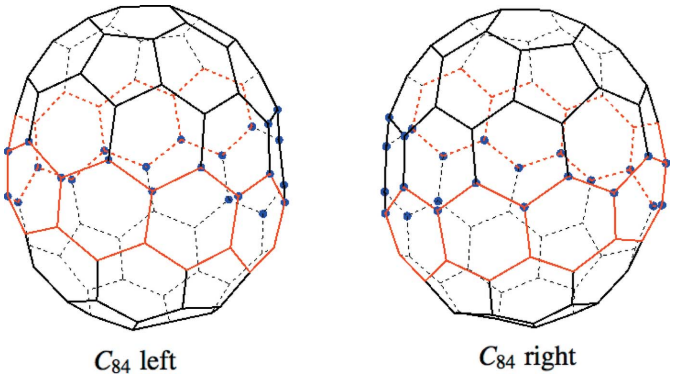

Figure 4
Left and right versions of C_{84} polytopes. The two versions differ by orientation of the inserted spiral belt with respect to the direction of α_2. Their pancake stacks coincide. Black circles indicate the 24 vertices that were added to C_{60}.

A flattened image of a one-loop spiral of eight hexagons is shown in Fig. 5. The pentagons at its extremes are either incorporated into a continuation of the loop, or are part of the original polytope before the insertion.

Left and right oriented spirals of polytopes $C_{108}, C_{132}, \ldots$ and nanotubes arise in a similar way as in the case of C_{84}. Each time the additional two rings of six hexagons (24 new vertices) can be inserted into the middle of the structure (see Fig. 6). The greater the number of pairs of hexagonal rings inserted, the longer the resulting nanotube that is built.

4. Concluding remarks

Breaking of the icosahedral symmetry of C_{60} to the subgroup $A_1 \times A_1$ is the most complicated of the three possible methods of constructing nanotubes through the repeated application of the symmetry-breaking mechanism. Indeed, in Bodner *et al.* (2013, 2014) an appropriate number of rings of hexagons and pentagons was inserted between the upper and lower halves of the C_{60} shell. In the present case a number of complete loops of a spiral of hexagons needs to be inserted between the upper and lower parts of C_{60}.

One may be interested in constructing open-ended nanotubes rather than nanotubes that are closed on both ends; new versatile possibilities occur. Thus one can start from a single layer of graphene, which is the sheet of hexagons in $\mathbb{R}^2$. Then cutting a strip of constant width from the graphene, one can wrap it on a surface of a cylinder of an appropriate radius. It is important that both sides of the strip pass through identical sets of graphene points to have them matched seamlessly on the surface of the cylinder. Such a requirement still leaves an infinite (discrete) number of possible radii of the cylinder. The direction of the strip is dictated by the direction of the roots of the reflection groups.

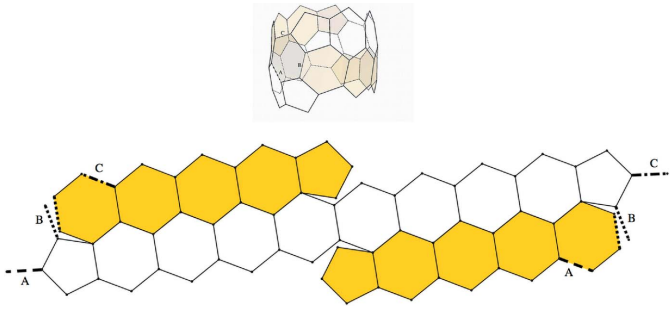

Figure 5
Flattened spiral that, added to C_{60}, transforms it to C_{84}. The three types of dashed lines indicate which edges are to be identified.

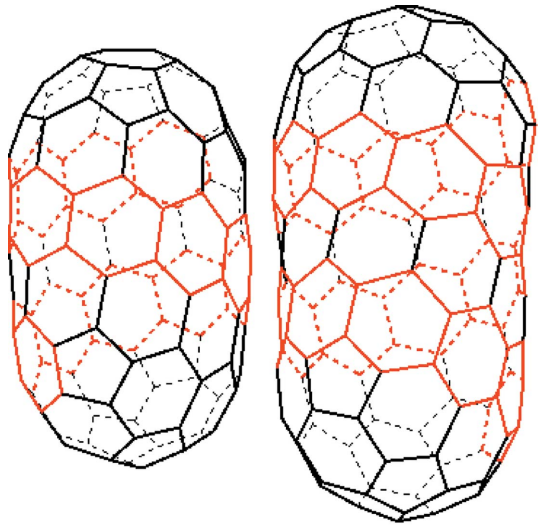

Figure 6
Left versions of the polytopes C_{108} and C_{132}, where multiple spiral belts (see Fig. 5) were added.

Fullerenes and related nanotubes are sometimes used as carriers for other molecules in their interior. Symmetry alone admits several possibilities of defining special positions within fullerenes. A systematic description of such cases would be of interest.

An independent, interesting viewpoint on the structure of the fullerenes is found in Kostant (1994, 1995).

Acknowledgements

The authors are grateful for partial support of the work by the Natural Sciences and Engineering Research Council of Canada and by the MIND Research Institute of Irvine, California. MS would like to express her gratitude to the Centre de Recherches Mathématiques, Université de Montréal, for the hospitality extended to her during her postdoctoral fellowship. She is also grateful to MITACS for partial support.

References

Bodner, M., Patera, J. & Szajewska, M. (2013). *Acta Cryst.* A**69**, 583–591.
Bodner, M., Patera, J. & Szajewska, M. (2014). *PLOS ONE*, 10.1371/journal.pone.0084079.
Champagne, B., Kjiri, M., Patera, J. & Sharp, R.T. (1995). *Can. J. Phys.* **73**, 566–584.
Fowler, P. W. & Manolopoulos, D. E. (1992). *Nature (London)*, **355**, 428–430.
Fowler, P. W. & Manolopoulos, D. E. (2007). *An Atlas of Fullerenes.* New York: Dover Publications, Inc.
Kostant B. (1994). *Proc. Natl Acad. Sci. USA*, **91**, 11714–11717.
Kostant B. (1995). *Notices of the AMS*, **42**, 959–968.
Zhang, B. I., Wang, C. Z., Ho, K. M., Xu, C. H. & Chan, C. T. (1993). *J. Chem. Phys.* **98**, 3095–3102.